

Validation of a newly developed cross-flow high temperature heat exchanger (HT-HE) using Multiphysics simulation

Max Rübsam¹, Martin Pitzer¹, Reinhold Altensen¹

¹University of Applied Sciences, Technische Hochschule Mittelhessen, Gießen

1 Abstract

Heat-exchangers are devices used to transfer heat between two or more fluids and can be found in both heating and cooling processes. At high temperatures during operation, thermal induced stresses occur and can lead to the failure of the device.

The Technische Hochschule Mittelhessen has, in cooperation with the company WK, started a research project for the development of a HT-HE, which is designed for operating temperatures up to 1100°C and the contact with aggressive chemical media.

In order to develop an efficient HT-HE regarding the heat recovery, semi analytical calculations have been carried out to optimize the geometry of the heat exchanger.

This study focusses on the validation of these semi-analytical calculations by using Multiphysics simulation. Due to the time costly simulation of transient fluid-structure-interactions (FSI) while taking high temperatures into account, special emphasis has been placed on the reduction of simulation time without losing accuracy.

Initially, a number of simplified models were set up to control the bug-free operation of the relatively new ICFD-Solver. It has been shown that the necessary workarounds, due to some implementation errors, only had a minor effect on the heat transfer.

Modifications have been added to the input data in order to significantly reduce simulation time without affecting the quality of results.

The results of the simulations done with LS-DYNA show a qualitatively good correlation with the semi analytical calculations and improve the understanding of the thermo- and fluid dynamic processes inside the HT-HE during operation.

2 Introduction

Nowadays, heat exchangers (HE) are used in a variety of applications in order to reduce energy consumption. With increasing operating temperatures, the thermal induced stresses become one of the main focusses during the design process of a HE. During a research project, a low stress design for a HT-HE was developed for operating temperatures up to 1100°C.

The concept of the HT-HE can be seen in Fig. 1. It essentially consists of three components: An inner- and an outer pipe and shovel shaped flow channels ("shovels") which connect the pipes. The outer pipe can be considered as fixed in bearings, while the inner pipe as freely stored. Because of this, the resulting strains of the material, especially the shovels, during operation can be compensated by torsion of the inner pipe around the longitudinal axis thus making it possible to reach higher operating temperatures.

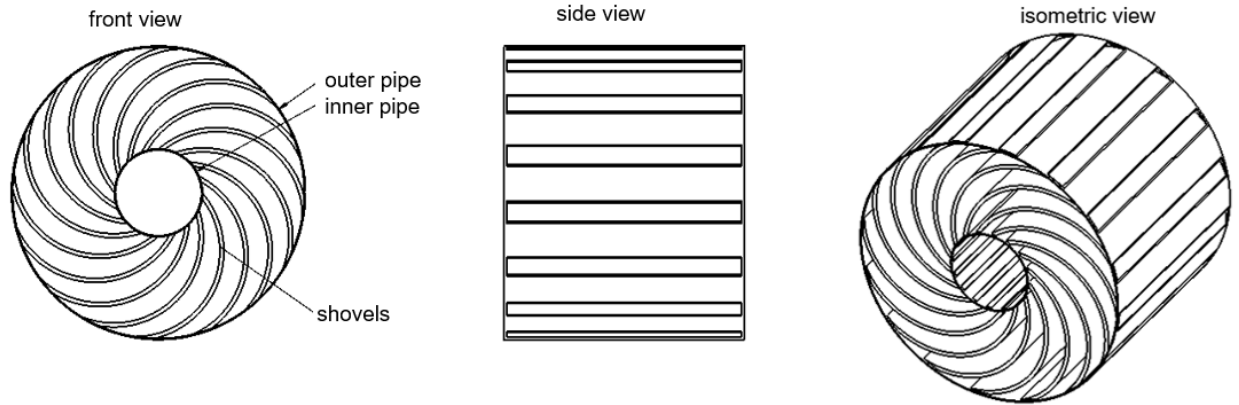


Fig.1: Structure of one half of the HT-HE

Furthermore, the HT-HE is designed in such a way, that a series connection is possible in order to increase the thermal efficiency. A series connection of two devices can be seen in Fig. 2.

The hot fluid flows linearly through the apparatus while the cold fluid enters the first set of shovels at the rear end of the apparatus from which it is led into the inner pipe. While still inside the inner pipe, it flows into the second half of the apparatus (3) and is led through the next set of shovels back to the outer pipe. From here, a connection piece allows the cold fluid to enter into the next apparatus where the procedure is repeated.

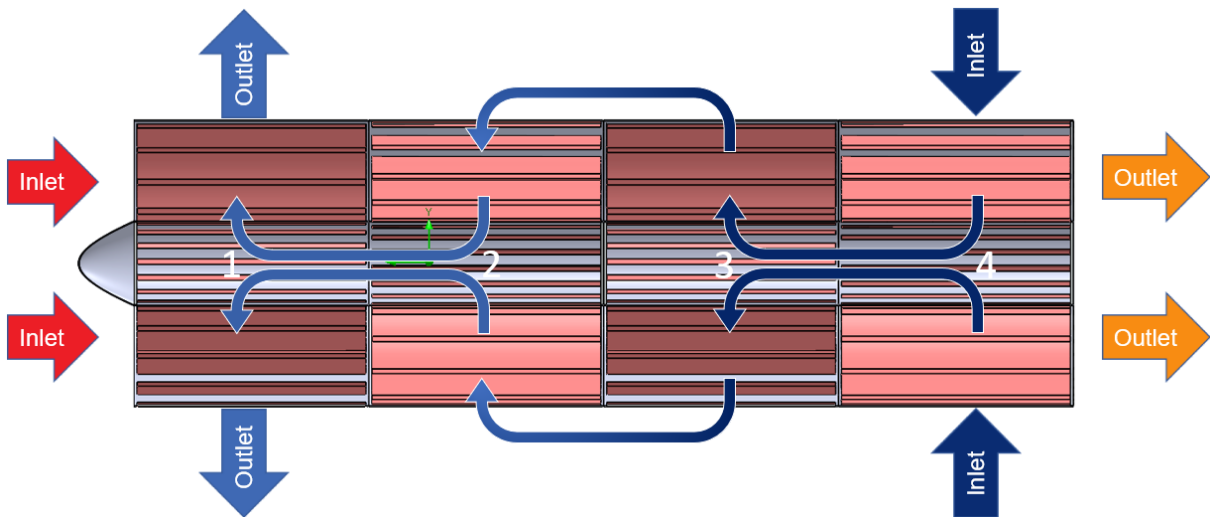


Fig.2: Flow control of two HT-HEs connected in a series

To analyze the thermal efficiency, semi-analytical simulations were carried out and temperature profiles for sections of the HT-HE were developed. These temperature profiles were then used to analyze the structural strength of the device using thermally/mechanically coupled FEM-computations.

In order to reduce the assumptions made in this two-step-process, numerical calculations of the fluid-structure interaction (FSI) under consideration of high temperatures had to be done.

Due to the large geometry of the HT-HE, the reduction of the computation time was important.

3 Fundamentals

When a viscous fluid flow is in contact with a solid, a velocity boundary layer forms at the interface. In addition to this, a thermal boundary layer exists as soon as there is a difference in temperature between the fluid and the solid.

The discretization of these boundary layers is crucial and a lot of information about the state of the flow has to be taken into account before a proper mesh can be created. In order to model the boundary layer, the dimensionless distance from the wall y^+ has been established. The y^+ -variable can be used to calculate the distance Δy of the first node to the wall.

$$\Delta y = \frac{y^+ \cdot \eta}{\rho \cdot u_\tau} \tag{1}$$

With η being the dynamic viscosity, ρ for the density and u_τ for the friction velocity which takes the Reynold number and the wall shear stress into consideration. Estimations for the friction velocity can be found in [1] and [2].

In order to be able to precisely resolve the heat transfer in the area close to the wall of a flow, a y^+ value of approx. one is recommended. [3]

For the simulation of the FSI, the solver for the solid and the fluid have to be coupled. In LS-DYNA a partitioned method is implemented were the user can choose between an explicit and an implicit coupled scheme. When heat transfer is also of interest, the thermal solver has to be added which is fully coupled with the ICFD thermal solver using a monolithic approach thus making it possible to investigate the exchange of thermal energy inside the HE. [4]

4 Methods

For the investigation of the FSI, the ICFD-Solver was chosen and all simulations were carried out using the version LS-DYNA R9.3. Due to the fact that the ICFD-Solver was implemented only recently, numerous test simulations were done to verify the proper functioning of the solver.

Therefore, a transient pipe flow was modelled and verified by an analytical calculation. The boundary conditions for the simulations are listed in table 1.

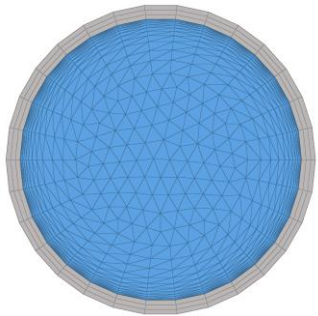
pipe length: 100 mm pipe diameter: 20 mm		
Initial temperature	20 °C	
T_{inlet}	120 °C	
v	1.0 m/s	
termination time	40 s	
y^+ -value	0.1	
material	DIN EN 1.4959 [5]	
number of nodes	3.12e+4	
number of elements	1.47e+5	

Fig.3: Front view of the pipe model

Table 1: Boundary conditions for the pipe flow

For the analytical calculation, the explicit Euler procedure was selected and carried out with Excel VBA. In order to determine the temperature profiles for the solid and the fluid as a function of time, the energy balance is set up for each section with consideration of the longitudinal heat conduction.

The resulting temperature profiles in dependency of the pipe length are shown in Fig. 4 for both the simulation and the analytical calculation at termination time.

The temperature profiles for the fluid section correspond qualitatively well while the temperature profiles for the solid deviate more. Especially at the inlet, higher temperatures appear regarding the simulation. One explanation for this is that within the analytical calculation the thermal start-up flow is not taken into account and the heat transfer coefficient is viewed as constant.

Nevertheless, the experiment proves that the expected results of the ICFD-solver in regard to the heat transfer can be viewed as physically plausible.

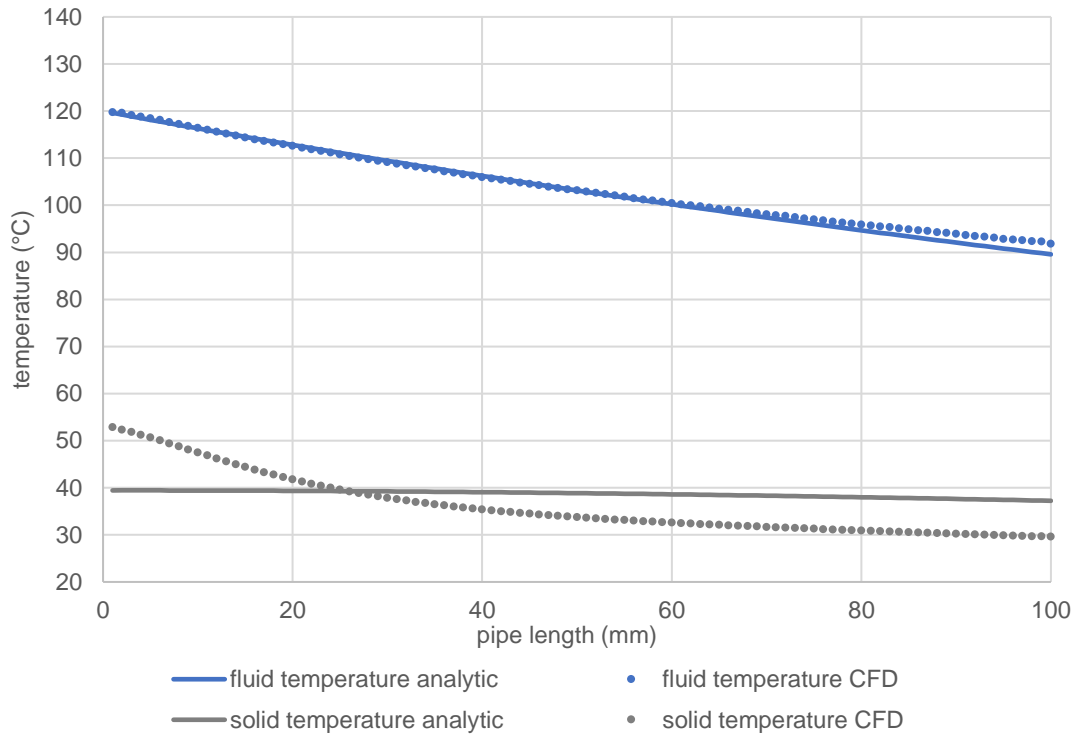


Fig.4: Comparison of the temperature calculation by CFD and analytic

For the next step, three-dimensional models of the inner pipe and the shovel were created and discretized. In Fig. 5, the solid (grey) and the segments of the 16 shovels (blue) at the inlet and outlet can be seen for the inner pipe. As well as the mesh for one single shovel with the domain for the hot fluid (red), the cold fluid (blue) and the solid (grey).

A previously conducted grid refinement study for the shovel with regard to the heat transfer showed that for an y^+ -value of 0.1, a grid-independent solution is achieved. [6]

This value could not be reached for the inner tube, due to the large dimensions and the necessary usage of turbulence models because of the high velocities and the fluid guidance. Therefore, a model with y^+ -values ranging from 5-10 was set up.

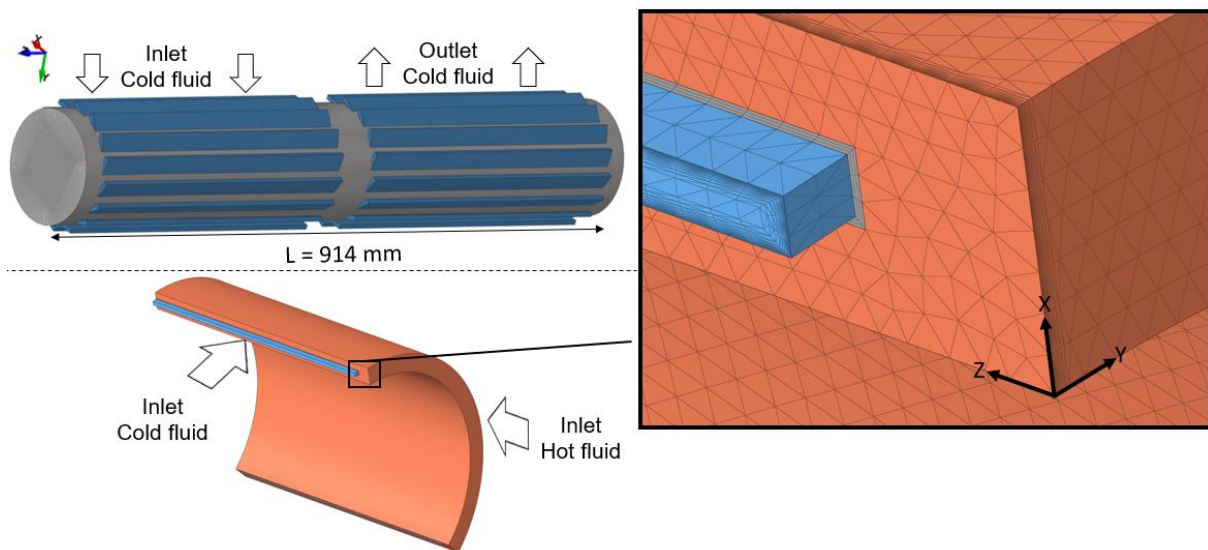


Fig.5: Isometric view of the models "inner pipe" and "shovel"

4.1 Boundary conditions

For an optimal simulation of stresses and strains, the boundary conditions should be selected as realistically as possible. When simulating a heat exchanger, this means taking the heating process into account. Ideally, the inlet temperatures of the cold and hot gas should be scaled as a function of time using a load curve. Depending on the heating speed, simulation times of 20-60 min would be achieved. With models of this size, computing times of several years would be the result for given computer capacities.

For this reason, simplifications must be made so that the computing time can be limited to a few weeks. Firstly, the boundary conditions for operation at full load are selected for both models and a quasi-stationary state is forced. This means that the termination time can be limited to a few minutes until a steady state is achieved.

The basis for the boundary conditions density, velocity and temperature is an iterative simulation program [7]. With the help of this program, inlet temperatures of the shovels as well as the average cold and hot gas velocities can be calculated. For the following simulation, an operating temperature of 600°C was chosen. For the exact boundary conditions chosen we refer to [6] chapter 4.6.

Since the implementation of different material cards for the respective flow domains was only successful for a shared memory parallel (SMP) system, but not in connection with a massively parallel processing (MPP) system, the material parameters of the fluids for the corresponding temperature range are averaged for the simulation.

Secondly, the density of the solid for the simulation of the shovel is reduced by a factor of 1000. By doing this, the necessary amount of thermal energy required to cause a temperature change in the solid can be reduced. The test simulations done, indicate that the scaling of the density, when considering thermal induced stresses, leads to approximately identical stress and temperature profiles. The required simulation time can be reduced depending on the scaling factor. As a result, simulation times of several tenths of a second are sufficient to achieve a steady state in the overall system. For a more detailed description see [6] appendix B.

Thirdly, for the simulation of the inner pipe, the domain of the hot fluid surrounding the inner pipe is neglected and a constant average temperature for the solid is determined. Due to the size of the geometry and the required mesh fineness when considering the heat transfer this simplification has to be made. Otherwise, the number of elements would surpass 2×10^7 by far. A model of this size, in combination with turbulence models, would exceed the available computing capacities considerably. Further limiting factors are that at the time of writing only transient simulations with tetrahedral elements, where no symmetry conditions for the flow domain can be defined, are supported by the ICFD-solver. For these reasons, the fluid domain of the hot fluid is not modelled, so that only the investigation of the cold gas side heat transfer is possible.

5 Results

5.1 Modell "Shovel"

Due to the simplifications made for the model, a steady state was reached after 0.55 s for which a computation time of around two weeks was necessary.

For the representation of the temperature profiles of the two fluid domains of the shovel, section planes in the central area of the model have been selected. The heat transfer from fluid to solid and vice versa, which takes place over the entire contact surface, can be seen in Fig. 6.

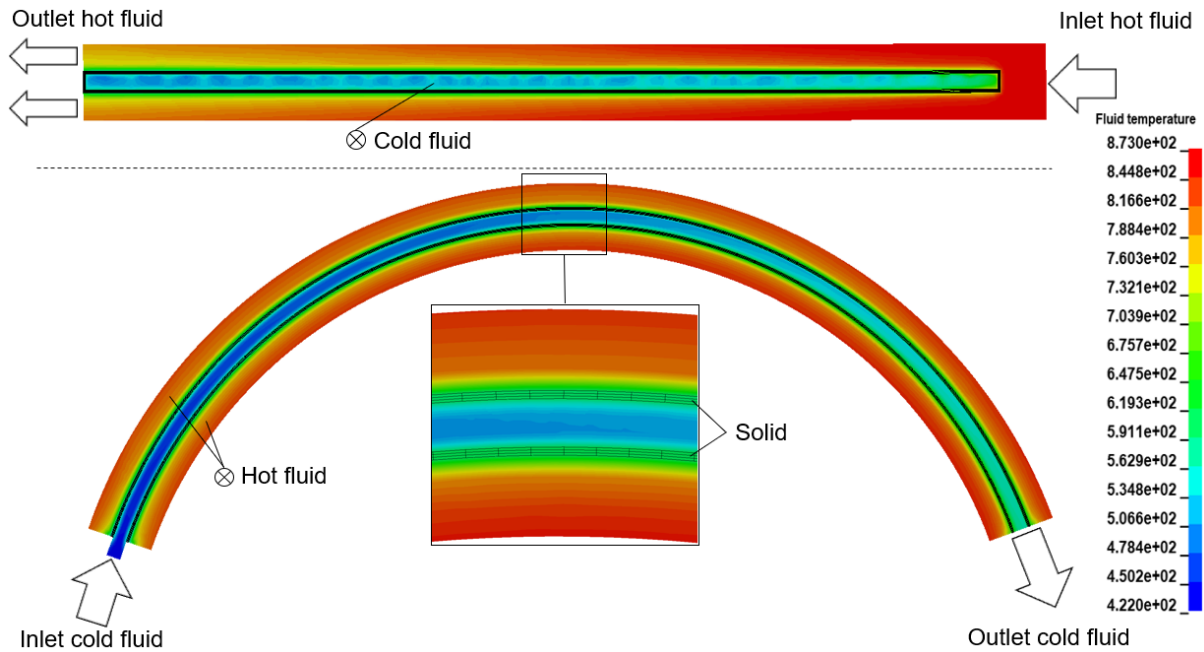


Fig.6: Temperature profiles of the fluid sections for the shovel

By weighting the temperatures at the outlet with the corresponding mass flow of the respective cell, an average temperature for the cold fluid and for the hot fluid can be determined [8]. On the basis of Eq. (2),

$$\Delta T_m = \frac{T_{cold}^{out} - T_{cold}^{in}}{\ln \left(\frac{T_{solid} - T_{cold}^{in}}{T_{solid} - T_{cold}^{out}} \right)} \quad (2)$$

and the Fourier's law [9], the heat flux and the heat transfer coefficient can be calculated

$$\dot{Q} = -\lambda \cdot A \cdot \frac{\partial T}{\partial y} = \alpha \cdot A \cdot \Delta T_m \quad (3)$$

which then allows a comparison with the semi-analytical calculations and can be seen in table 2.

	CFD	analytical	CFD	analytical
	α [W/(m ² K)]		\dot{Q} [kW]	
hot fluid	44.9	29.0 – 50.2	≈ 50.8	53.2 – 57.6
cold fluid	20.8	18.2		

Table 2: Heat transfer coefficient for the shovel (CFD and analytical solution)

A good correlation between the results can be observed. Nevertheless it has to be mentioned that the effect of the inner tube on the heat flux is neglected for the calculation of the heat flux in the numerical analysis.

The temperature profile of the solid is shown in Fig. 7 and corresponds quantitatively to the expected temperature profile for a cross-flow. The highest temperatures of 815 K are found in cell 3;1, since the maximum cold and hot gas temperatures occur in this area. In direction of cell 1;3, the fluid temperatures drop down to a minimum 508 K.

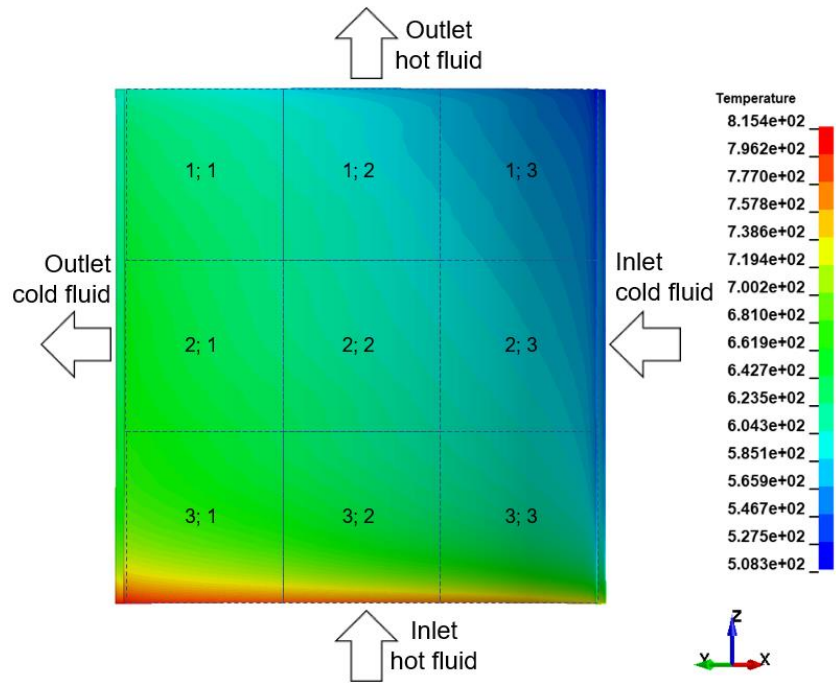


Fig.7: Temperature profile of the solid with regard to the shovel

By averaging the temperatures of the respective cell, comparability with the analytically calculated temperatures of the iterative simulation program can be achieved. Table 3 shows the temperatures in the comparison, as well as the difference in temperature between the calculation methods for the respective cell.

temperatures (K) of the individual cells of both calculation methods

CFD			Analytical			difference					
cell	1	2	3	cell	1	2	3	cell	1	2	3
1	612	581	562	1	621	596	569	1	-9	-15	-7
2	631	599	583	2	639	613	585	2	-8	-14	-2
3	679	643	620	3	658	632	603	3	20	10	17

Table 3: Comparison of the temperatures for the solid for both calculation methods

The comparison shows good overall quantitative and qualitative correlation. The numerical calculation indicates higher temperatures at the inlet of the hot fluid (cell 3;1, 3;2, 3;3) and lower temperatures in the adjacent areas.

The higher temperatures occurring near the inlet of the hot fluid can be explained by the section of the solid which is hit directly by the hot fluid. At this point, the highest temperatures occur, which are not taken into account by the iterative simulation program.

The thermally induced stresses are shown in Fig. 8. The maximum stresses of 90 MPa occur in the corner area of cell 3;3 and are caused by the flow guidance. Due to this, the highest temperature gradient between the two fluids is located here.

The increased stresses in the area of the inlet of the cold fluid are due to the bearing arrangement through which the contact with the outer pipe is taken into account. In general, an inhomogeneous stress profile, with stresses primarily in the range of 10-50 MPa can be observed.

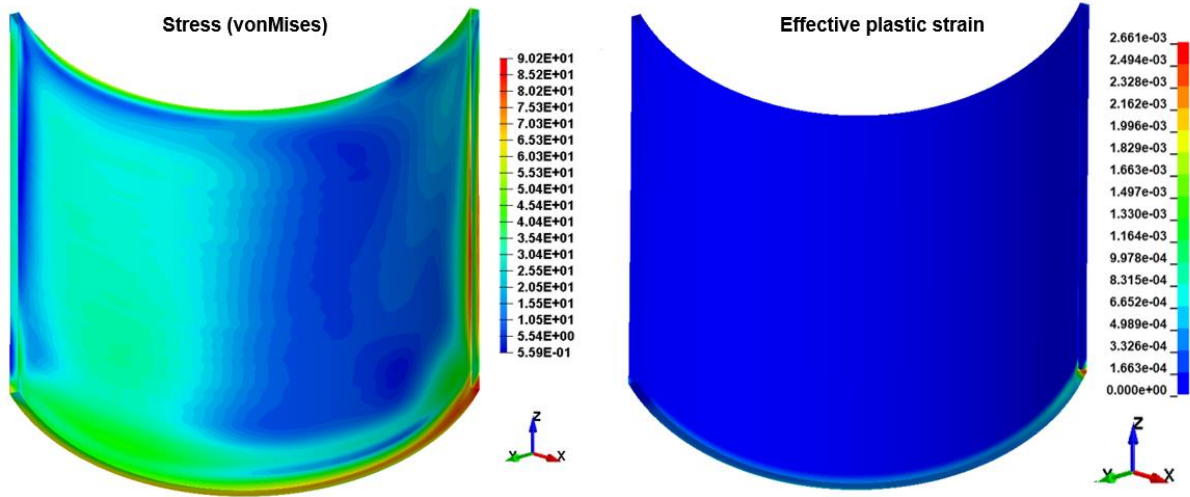


Fig.8: Stress and strain profiles of the shovel

Due to the stresses, plastic strains occur in the lower part of the solid. These are due to the high temperature gradient at the beginning of the calculation, which is present in this area as soon as the hot fluid reaches the solid, but the colder fluid has not yet warmed up. The high stresses at the beginning of the calculation are thus due to the selected boundary conditions and are below the yield stress if a heating phase is taken into account.

The only exception is the corner area in cell 3;3, in which stresses beyond the yield stress are also present in the stationary state. The maximum plastic strain is 0.26 %.

Due to the qualitatively good agreement of the analytically calculated temperature distribution with the results of the simulation, the results can be viewed as plausible.

5.2 Modell "Inner pipe"

For this model, a steady state was reached after 0.8 s. The velocity profile can be seen in Fig. 9. The upper section view is centered in the yz plane. The other two views show the streamlines in both directions through the middle area (middle picture) of the inner pipe and starting from an inlet surface (lower picture). The flow area is illustrated in grey.

Here it can be observed that the fluid which enters the inner pipe near the left edge has a relatively long resting time at the end face where it enters the middle part of the flow. In the lower two views, the resulting spin of the flow can be seen. Here, a forced redirection of the fluid occurs when re-entering the next set of shovels, which results in a backflow inside the shovels and leads to relatively high pressure losses.

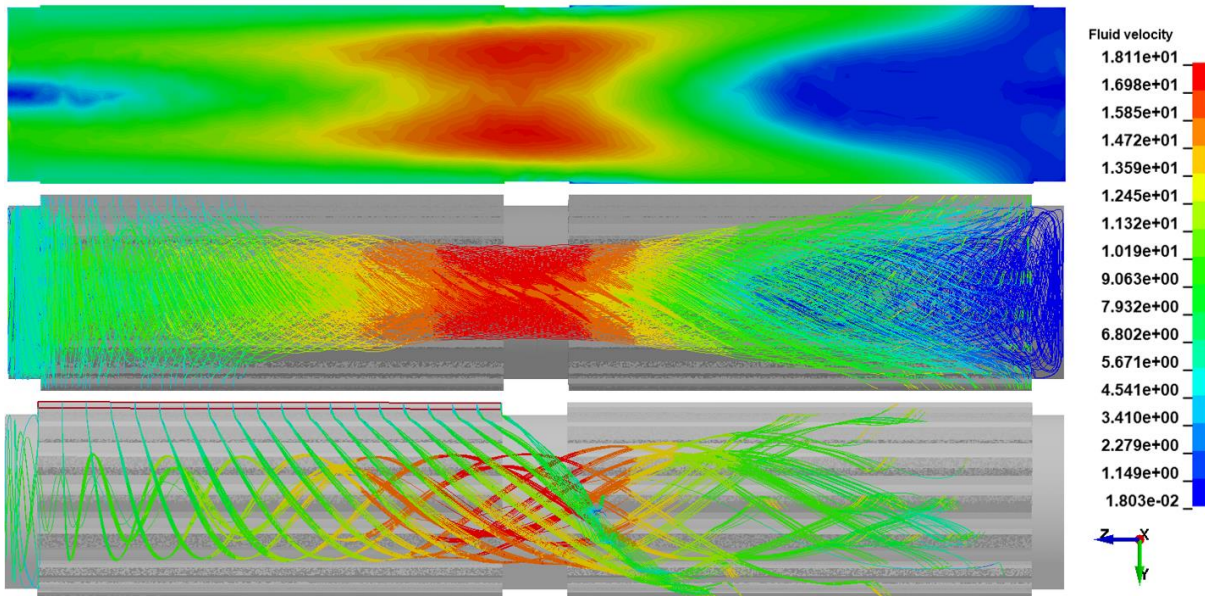


Fig.9: Velocity profile of the inner pipe

Due to the long resting time at the end face, higher temperatures occur in this area (see Fig. 10), as the heat is dissipated slower in the longitudinal direction of the pipe. In addition, a relatively large dead zone occurs at the opposite end face, which also results in long resting times and higher temperatures.

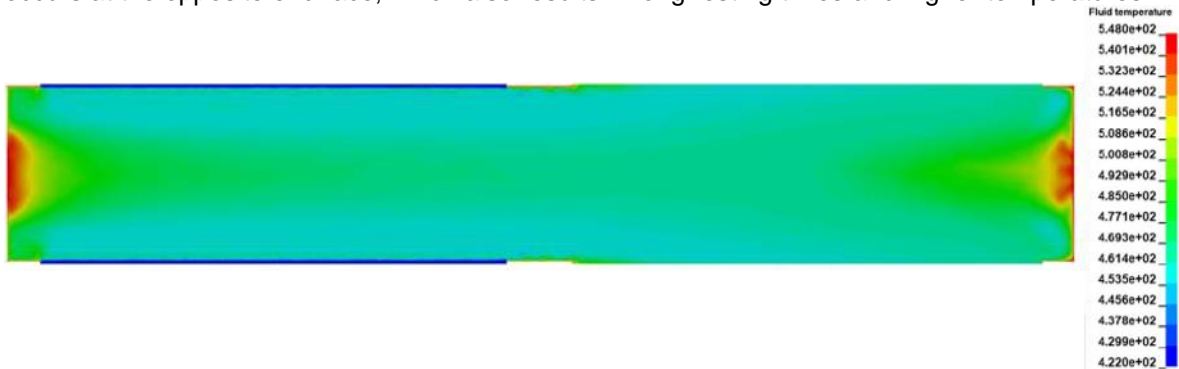


Fig.10: Temperature profile of the inner pipe

Similar to the shovel, the heat flux $\dot{Q} \approx 7.0$ kW and the average heat transfer coefficient $\alpha \approx 180$ W/m²K can be determined using the formulas (2) and (3). Due to the high y^+ -value, the calculated values can be interpreted as too high. Based on a total heat flux of approx. 54 kW, determined by the iterative simulation program, the heat transfer in the inner pipe can therefore be classified as relatively low. This can be explained by the small heat transfer area and the large dead zones.

6 Summary

The present paper focusses on the heat transfer between fluid and solid of selected parts of a HE, as well as the development of possibilities to reduce the computing time. In addition, information regarding the flow guidance inside the apparatus is obtained.

Firstly, the proper functioning of the ICFD-solver was investigated by simulation the transient heat transfer inside a simple pipe-model and comparing it with an analytical calculation. It could be shown that the assumptions made only lead to minor errors and that the results obtained can be regarded as physically reasonable.

In the following, the components "inner tube" and "shovel" were selected for the numerical calculation. For the latter, a mesh refinement study was carried out with the result that a y^+ -value of 0.1 would be ideal for in this model. Furthermore, it could be shown that by scaling the density of the solid the calculation time can be significantly reduced while maintaining the quality of the results.

The initial conditions for both models were chosen in such a way that a quasi-stationary state exists at the beginning of the simulation, which also results in a reduction of the computation time. The necessary boundary conditions for the models were determined by an iterative simulation program.

The evaluation of the shovel proved that the simulation corresponds qualitatively well with the analytical calculation regarding the heat transfer. The stresses in the solid result mostly in elastic deformation. The areas in which plastic deformation occurs are largely due to the neglect of the heating-up phase or do not exceed 0.24 %. Under the assumption that the free expansion of the shovels is made possible by the torsion of the inner pipe, it can be assumed that higher operating temperatures are unproblematic.

Due to the size of the inner pipe and the flow guidance, it was not possible to calculate a grid-independent solution with regard to heat transfer for the inner pipe. The heat flux can therefore be classified as too high. In comparison with the shovels, the heat flux inside the inner pipe thus plays a subordinate role, which is why future optimizations with regard to the heat transfer should be carried out in the area of the shovels.

With regard to the flow guidance, it was shown that a relatively high pressure loss is to be expected due to the forced redirection in the inner tube. This can be prevented by altering the arrangement of the shovels in the rear part of the apparatus.

7 Literature

- [1] Schlichting, H. : "Boundary-Layer Theory", Seventh edition, 1979, 641-642
- [2] von Karman, T. : "Turbulence and Skin Friction". J of the Aeronautical Sciences, Vol.1, 1934, 1-20
- [3] ANSYS I : "ANSYS CFX-Solver Theory Guide", 2009, 89
- [4] LSTC® Facundo Del Pin and LSTC® Rodrigo R. Paz : "ICFD THEORY MANUAL: Incompressible Incompressible fluid solver in LS-DYNA", 2014, 18-27
- [5] VDM Metals GmbH 2017 : "Alloy 800 H/HP", Werkstoffdatenblatt Nr. 4129, 2017, 4-5
- [6] Rüksam, M. „Numerische Berechnung der Fluid-Struktur-Interaktion unter Berücksichtigung hoher Temperaturen am Beispiel eines Hochtemperatur-Wärmeübertragers“, Master Thesis, University of Applied Sciences Gießen, 2019, 39-43
- [7] Holy, F. : "Simulation der stationären Betriebscharakteristik eines Radial-Kreuzstrom-Wärmeübertragers ", Master Thesis, University of Applied Sciences Gießen, 2019, 29-46
- [8] Gesellschaft Verfahrenstechnik und Chemieingenieurwesen : "VDI-Wärmeatlas" 11th edn, 2013, 28"
- [9] Fourier, JBJ. : "Théorie Analytique de la Chaleur", Reprint (2009) Cambridge University Press, 1st edition, 1822